Neuroscience 304 (2015) 198–208

DIFFERENTIAL CEREBELLAR $GABA_A$ RECEPTOR EXPRESSION IN MICE WITH MUTATIONS IN $CA_V2.1$ (P/Q-TYPE) CALCIUM CHANNELS

S. KAJA, [a,b,c,d*†] **A. J. PAYNE,** [c,d†] **E. Ø. NIELSEN,** [b‡] **C. L. THOMPSON,** [e¶] **A. M. J. M. VAN DEN MAAGDENBERG,** [f] **P. KOULEN** [c,g] **AND T. P. SNUTCH** [a]

[a] *Michael Smith Laboratories and the Djavad Mowafaghian Centre for Brain Health, University of British Columbia, 301-2185 East Mall, Vancouver, BC V6T 1Z4, Canada*

[b] *NeuroSearch A/S, Pederstrupvej 93, 2750 Ballerup, Denmark*

[c] *Vision Research Center, Department of Ophthalmology, University of Missouri – Kansas City, School of Medicine, 2411 Holmes Street, Kansas City, MO 64108, USA*

[d] *K&P Scientific LLC, 8570 N Hickory Street Suite 412, Kansas City, MO 64155, USA*

[e] *School of Biological Sciences, Durham University, South Road, Science Laboratories, Durham DH1 3LE, United Kingdom*

[f] *Departments of Human Genetics & Neurology, Leiden University Medical Centre, Einthovenweg 20, PO Box 9600, 2300 RC Leiden, The Netherlands*

[g] *Department of Basic Medical Science, University of Missouri – Kansas City, School of Medicine, 2411 Holmes Street, Kansas City, MO 64108, USA*

Abstract—Ataxia is the predominant clinical manifestation of cerebellar dysfunction. Mutations in the human *CACNA1A* gene, encoding the pore-forming α_1 subunit of $Ca_V2.1$ (P/Q-type) calcium channels, underlie several neurological disorders, including Episodic Ataxia type 2 and Familial Hemiplegic Migraine type 1 (FHM1). Several mouse mutants exist that harbor mutations in the orthologous *Cacna1a* gene. The spontaneous *Cacna1a* mutants *Rolling Nagoya* (tg^{rol}), *Tottering* (*tg*) and Leaner (tg^{la}) mice exhibit behavioral motor phenotypes, including ataxia. Transgenic knock-in (KI) mouse strains with the human FHM1 R192Q and S218L missense mutations have been generated. R192Q KI mice are non-ataxic, whereas S218L KI mice display a complex behavioral phenotype that includes cerebellar ataxia. Given the dependence of γ-aminobutyric acid type A ($GABA_A$) receptor subunit functioning on localized calcium currents, and the functional link between GABAergic inhibition and ataxia, we hypothesized that cerebellar $GABA_A$ receptor expression is differentially affected in *Cacna1a* mutants and contributes to the ataxic phenotype. Herein we quantified functional $GABA_A$ receptors and pharmacologically dissociated cerebellar $GABA_A$ receptors in several *Cacna1a* mutants. We did not identify differences in the expression of $GABA_A$ receptor subunits or in the number of functional $GABA_A$ receptors in the non-ataxic R192Q KI strain. In contrast, tg^{rol} mice had a ∼15% decrease in the number of functional $GABA_A$ receptors, whereas S218L KI mice showed a ∼29% increase. Our data suggest that differential changes in cerebellar $GABA_A$ receptor expression profile may contribute to the neurological phenotype of cerebellar ataxia and that targeting $GABA_A$ receptors might represent a feasible complementary strategy to treat cerebellar ataxia. **© 2015 IBRO. Published by Elsevier Ltd. All rights reserved.**

Key words: gamma aminobutyric acid receptor type A, cerebellar ataxia, *Cacna1a*, pharmacology, Familial Hemiplegic Migraine.

INTRODUCTION

Cerebellar ataxias are a diverse group of movement disorders and the predominant manifestation of acquired and inherited neurological diseases affecting cerebellar structure and function (Kotagal, 2012; Pandolfo and Manto, 2013). Mechanistically, ataxia is caused by aberrant cerebellar Purkinje cell (PC) firing (Womack et al., 2004; Walter et al., 2006). Episodic Ataxia type 2 (EA-2; OMIM #108500) is the most common manifestation of Episodic Ataxia (Jen et al., 2007), and defined by the presence of mutations in *CACNA1A* (Ophoff et al., 1996), the gene encoding the pore-forming α_1 subunit of voltage-gated $Ca_V2.1$ (P/Q-type) Ca^{2+} channels. Other mutations in *CACNA1A* cause Familial Hemiplegic Migraine type 1 (FHM1), Spinocerebellar Ataxia type 6 and rare forms of epilepsy (Ophoff et al., 1996; Zhuchenko et al., 1997; Jouvenceau et al., 2001; Imbrici et al., 2004; de Vries et al., 2009).

Several mouse models exist that carry mutations in the orthologous mouse *Cacna1a* gene. Most of these mutants, including *Tottering* (*tg*), *Rolling Nagoya* (tg^{rol}) and *Leaner* (tg^{la}), arose spontaneously and display complex phenotypes of cerebellar ataxia, often paired with absence epilepsy and/or other motor phenotypes such as dyskinesia and dystonia (Green and Sidman, 1962; Oda, 1973; Herrup and Wilczynski, 1982). In addition, transgenic knock-in (KI) mouse models were

*Corresponding author. Present address: Loyola University Chicago, Stritch School of Medicine, Department of Ophthalmology, 2160 First Avenue, Maywood, IL 60153, USA.
E-mail address: skaja@luc.edu (S. Kaja).
† Authors contributed equally to this study.
‡ Present address: Xellia Pharmaceuticals ApS, Dalslandsgade 11, 2300 Copenhagen S, Denmark.
¶ Deceased.

Abbreviations: EA-2, Episodic Ataxia type 2; FHM1, Familial Hemiplegic Migraine type 1; $GABA_A$, γ-aminobutyric acid type A; KI, knock-in; PC, Purkinje cell; qPCR, quantitative polymerase-chain reaction; *tg*, Tottering; tg^{la}, Leaner; tg^{rol}, Rolling Nagoya.

http://dx.doi.org/10.1016/j.neuroscience.2015.07.044
0306-4522/© 2015 IBRO. Published by Elsevier Ltd. All rights reserved.

generated which harbor the human FHM1 missense mutations R192Q (R192Q KI) and S218L (S218L KI) in the *Cacna1a* gene (van den Maagdenberg et al., 2004, 2010). R192Q KI do not display a motor phenotype of ataxia (van den Maagdenberg et al., 2004), similar to patients with the same mutation (Ophoff et al., 1996). In contrast, S218L KI show a complex behavioral and synaptic phenotype that includes cerebellar ataxia (van den Maagdenberg et al., 2010; Gao et al., 2012), analogously to patients with this mutation (Kors et al., 2001; Stam et al., 2009).

The rationale for the present study was based on the functional link between neuronal Ca^{2+} influx and γ-aminobutyric acid type A ($GABA_A$) receptor subunit expression (Hansen et al., 1992; Gault and Siegel, 1997, 1998; Houston et al., 2007, 2008), as well as on the loss of GABAergic inhibition as etiological basis for ataxia (Egawa et al., 2012). Notably, abnormalities in cerebellar $GABA_A$ receptor expression have been found in essentially all natural $Ca_V2.1$ mutants studied so far. For instance, $\alpha_6\beta_{2/3}\gamma_2$ subunit-containing receptors are reduced by ~40% in cerebellar granule cells of *tg* mice (Kaja et al., 2007a). Similarly, tg^{la} mice exhibit a reduced ability for producing dorsal root potentials, which might implicate GABAergic cerebellar interneurons (Ogasawara et al., 2001).

We, therefore, hypothesized that (1) $GABA_A$ receptor abnormalities in the cerebellum are only present in conjunction with a motor phenotype of ataxia, and are not a common feature among all $Ca_V2.1$ mutant mice, and (2) that gain- and loss-of-function *Cacna1a* mutations are associated with differential $GABA_A$ receptor abnormalities.

EXPERIMENTAL PROCEDURES

Animals

The transgenic mouse strains FHM1 R192Q KI and FHM1 S218L KI were generated at the Leiden University Medical Centre, Leiden, The Netherlands (van den Maagdenberg et al., 2004, 2010). Heterozygous breeder pairs were maintained at the University of British Columbia, Dept. of Zoology vivarium, on a 12-h light/dark cycle with food and water available *ad libitum*. Animals used for experiments were 2–3 months of age. All experiments were approved by the University of British Columbia Animal Care Committee (license no. A07-0036) and in accordance with respective national and university guidelines. Tissue from *Rolling Nagoya* mice was provided by Drs. Jaap Plomp and Arn van den Maagdenberg (Leiden University Medical Center, Leiden, The Netherlands). *Tottering* mice were maintained at the vivarium at Durham University, School of Biological Sciences and obtained from Jackson Laboratories (Bar Harbor, ME).

Quantitative polymerase-chain reaction (qPCR)

Wild-type and homozygous R192Q KI littermates were euthanized by cervical dislocation and forebrain (without olfactory bulb) and cerebellum were dissected into 0.1 M ice-cold phosphate-buffered saline (pH 7.4) and subsequently snap frozen in liquid nitrogen. RNA was extracted using Trizol® reagent (Invitrogen, Burlington, ON, USA) according to the manufacturer's recommendation. Briefly, tissue was homogenized in 1 mL Trizol® reagent. Following centrifugation (12,000×*g*, 10 min, 4 °C), 200 µL chloroform was added and phases separated by centrifugation (12,000×*g*, 15 min, 4 °C). RNA was precipitated from the aqueous phase by addition of 500 µL isopropyl alcohol. Following centrifugation (12,000×*g*, 15 min, 4 °C) the pellet was washed with 1 mL 70% ethanol and centrifuged (7500×*g*, 5 min, 4 °C). RNA was eluted in 50 µL DEPC-treated water. RNA concentrations were determined spectrophotometrically.

cDNA was synthesized from total RNA using the High-Capacity cDNA Reverse Transcription Kit (Applied Biosystems, Foster City, CA, USA) according to the manufacturer's recommendations.

qPCR was performed using a 7500 Real-Time PCR System and gene-specific Taqman® gene expression assays (both from Applied Biosystems, Foster City, CA, USA) using a total reaction volume of 25 µL. Mouse β-actin (ACTB) was used as endogenous control and in parallel on every plate. We performed relative expression analysis. Data were analyzed using the System SDS Software Version 1.3.1.21 (both from Applied Biosystems, Foster City, CA, USA), and subsequently exported and plotted in SigmaPlot. Statistical significance was performed using the $2^{-\Delta\Delta CT}$ method for relative gene expression data (Livak and Schmittgen, 2001; Bustin et al., 2009).

Quantitative immunoblotting

Immunoblotting was performed using SDS–PAGE on 4–12% NuPAGE® Novex® Bis-Tris Mini Gels (Invitrogen, Carlsbad, CA, USA) under reducing conditions (20 µg protein/gel lane).

Commercially available anti-$GABA_A$ receptor subunit-specific antibodies were used at the following concentrations: anti-α1 (Chemicon, Temecula, CA, USA; cat AB5946; dilution 1:3000); anti-α_6 (Abcam, Cambridge, MA, USA; catalog # ab8338; dilution 1:2000); anti-$\beta_{2/3}$ (EMD Millipore, Bellerica, MA, USA; clone 62-3G1; catalog # 05-474; dilution 1:500); anti-γ_2 (Santa Cruz Biotechnology, Santa Cruz, CA, USA; catalog # sc-101963; dilution 1:200); anti-δ (Santa Cruz Biotechnology, Santa Cruz, CA, USA; catalog # sc-25705; dilution 1:400); anti-actin (Millipore, Temecula, CA, USA; catalog # MAB1501R; dilution 1:50,000). ECL™-HRP-linked secondary antibodies (goat anti-rabbit, sheep anti-mouse and donkey anti-goat) were obtained from GE Healthcare (Piscataway, NJ, USA) and used at 1:10,000 dilution. Immunoreactive species were detected using the enhanced chemiluminescence Western Lightning Plus kit (Perkin Elmer, Waltham, MA, USA) and exposure to CL-XPosure light-sensitive film (Thermo Scientific, Rockford, IL, USA).

All antibodies have previously been validated in the published literature (Mehta and Ticku, 1999; Kang et al., 2006; Kaja et al., 2007a; Matsuoka et al., 2008) and were

tested for their specificity using transient overexpression of individual $GABA_AR$ subunits (data not shown).

Protein quantification was performed essentially as described previously (Kaja et al., 2007a). Films were scanned using a commercial scanner at 1200-dpi resolution, and immunoblots quantified using ImageJ software (NIH, Bethesda, MD, USA). Calibration curves of the antibody response for a range of antigen concentrations were determined following immunoblotting and the linear range of the detection system established.

Experiments were designed such that the immunoreactivities obtained in the assays were within this linear range, thus permitting the direct comparison of the amount of antigen applied per gel lane between samples. Cerebellar lysates from five animals (R192Q KI vs. wildtype) or three animals (tg^{rol} vs. wild-type) were run on the same gel. Each experiment was repeated three times, and data are presented as mean ± s.e.m. for those three experiments.

[^{3}H] Radioligand autoradiography

[^{3}H] Ligand autoradiography on whole brain sections was performed as described previously (Kaja et al., 2007a). Cryostat sections (14 μm) from frozen, non-fixed adult mouse brains (control and R192Q KI) were preincubated in 10 mM Tris–HCl, pH 7.4, and 0.15 M NaCl for 15 min at 0 °C for [^{3}H] Ro15-4513 and [^{3}H] Ro15-1788 binding assays and 0.31 M Tris–citrate solution, pH 7.1, for [^{3}H] muscimol binding assays. Incubations with ligands used fresh buffers of composition identical to those used for the preincubations. In order to highlight γ_2 subunit-containing receptors, [^{3}H] Ro15-4513 (20 nM) was used with and without 10 μM flunitrazepam for a 90-min incubation at 0 °C, followed by three 5-s washes in 10 mM Tris–HCl, pH 7.4, and 50 mM NaCl, a dip in distilled water, and followed by rapid drying. The non-specific binding of [^{3}H] Ro15-4513 was defined in the presence of 10 μM flumazenil (Ro15-1788; Hoffmann-La Roche, Basel, Switzerland). The same conditions and washes were used for the analysis of the GABA binding site, employing [^{3}H] muscimol (20 nM) as radioligand in the absence (total binding) and presence (non-specific binding) of 1 mM GABA. The sections were washed three times for 5 s in 10 mM Tris–citrate, pH 7.1, followed by dipping in distilled water and air drying. Sections were exposed to Hyperfilm-3H (Amersham International, GE Healthcare UK, Chalfont, Buckinghamshire, UK) for periods of between 5 days and 6 weeks, depending on the ligand used. Images were produced by scanning the film using a commercial scanner at a resolution of 1200 dpi. Quantification was performed using ImageJ software (NIH, Bethesda, MD, USA). Across the entire granule cell layer of the cerebellum, 15 squares of 4 × 4 pixels in size were placed and the mean density determined. The mean background of the film was determined similarly, using three squares of 4 × 4 pixels, the mean density of which was subsequently subtracted from the mean obtained from measurements in the CGC layer to yield the specific mean density. [^{3}H] Microscales were purchased from Amersham International. Densitometry was performed using ImageJ software and a standard curve generated was used to confirm that signals were within the linear range of the film.

[^{3}H] Radioligand binding assays

[^{3}H] Radioligand binding was essentially performed as described previously (Kaja et al., 2007a). Briefly, mice were euthanized by cervical dislocation and the forebrain (without olfactory bulb) and cerebellum were dissected into 0.1 M ice-cold phosphate-buffered saline (pH 7.4) and subsequently snap frozen in liquid nitrogen. Tissue was thawed on ice in 50 volumes assay buffer (50 mM Tris–citrate pH 7.3 for [^{3}H] muscimol binding, 50 mM Tris–HCl pH 7.4 for [^{3}H] R015-4513 and [^{3}H] Ro15-1788 binding). Samples were homogenized in a Dounce tissue grinder and centrifuged at 15,000 rpm in a Sorvall ultracentrifuge at 5 °C (rotor SM-24). The pellet was washed twice in 50 volumes assay buffer and re-homogenized. In order to release endogenous neurotransmitter, tissue was incubated for 30 min in 37 °C water bath and re-centrifuged. The pellet was then resuspended in 50 volumes assay buffer, flash frozen in liquid nitrogen and stored overnight at −20 °C. Immediately prior to experiments, tissue was thawed in RT water bath, centrifuged and the pellet resuspended 200-fold for [^{3}H] muscimol experiments and 500-fold for [^{3}H] R015-4513 and [^{3}H] Ro15-1788 binding. Protein concentrations of membrane preparations were determined by the method of Lowry (Lowry et al., 1951) employing bovine serum albumin as the standard protein for calibration.

Data analysis and statistics

Data throughout this manuscript are presented as mean ± s.e.m., except the relative gene expression level (R_Q), where error bars designate R_{Qmin} and R_{Qmax}, in accordance with MIQE guidelines (Bustin et al., 2009). Throughout the manuscript, *n* refers to the number of individual animals tested per group. Prism software v6 (GraphPad Software Inc., La Jolla, CA, USA) was used for statistical analysis and generation of histograms in Figs. 1 and 2. Radioligand binding data were analyzed in SigmaPlot v10 (Systat Software, Inc., San Jose, CA, USA), using the one-binding site regression tool with 200 iterations. Overall B_{max} and K_D values were obtained by calculating the mean values obtained from each individual animal. Rosenthal transformations were performed on radioligand binding data and plotted as Scatchard plots for illustration purposes only (Thompson et al., 1998; Payne et al., 2006; Kaja et al., 2007a).

Statistically significant differences were tested for using Student's *t*-tests, as appropriate. Statistical significance was defined as $P < 0.05$.

RESULTS

Non-ataxic R192Q KI have normal cerebellar $GABA_A$ receptor expression

In order to determine whether altered cerebellar Ca^{2+} homeostasis resulting from the R192Q mutation affects transcription of cerebellar $GABA_A$ receptor subunits, we performed qPCR on cDNA from wild-type and

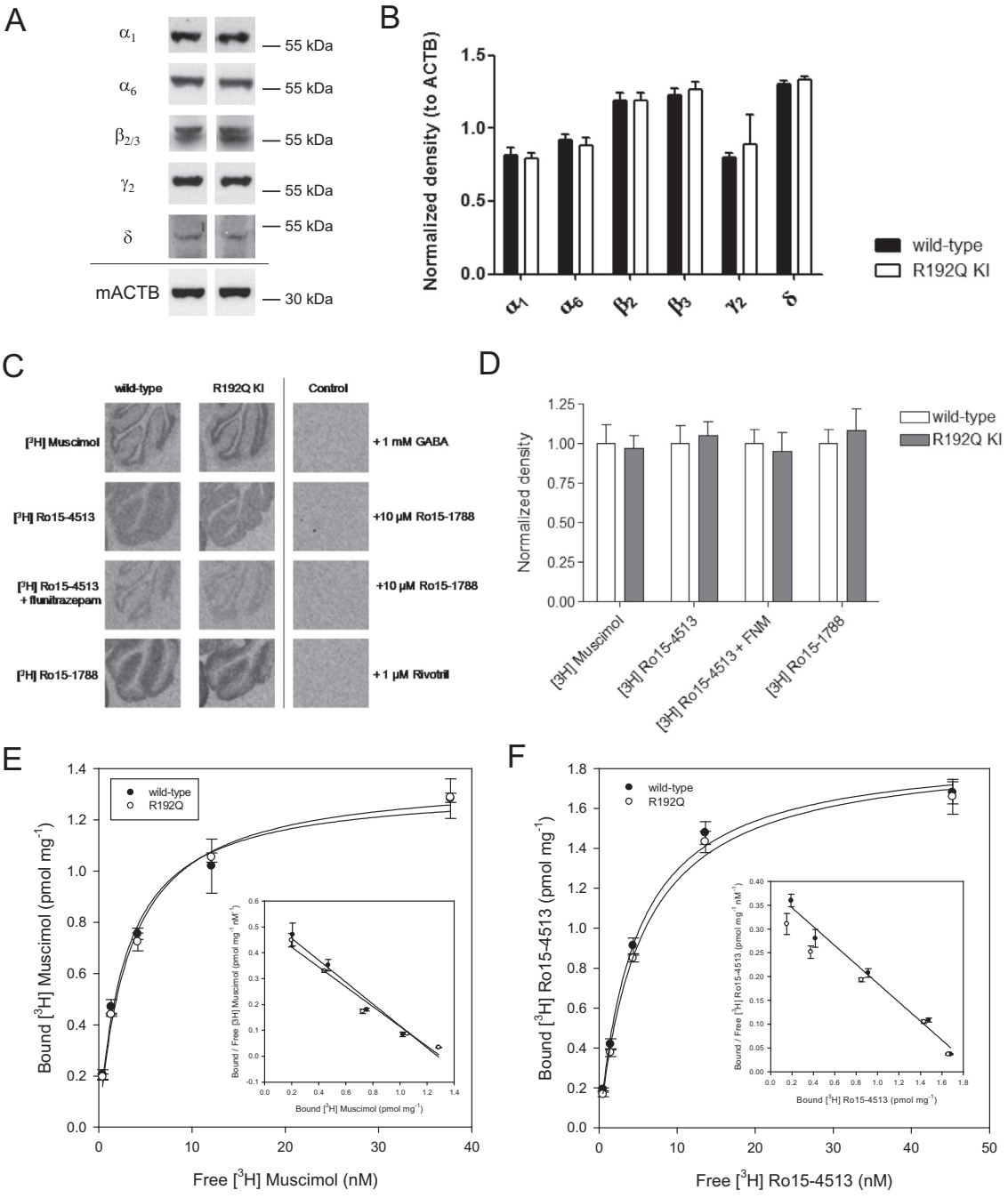

Fig. 1. (A) Representative immunoblot for $GABA_AR$ subunit expression in the cerebellum. (B) Quantification revealed no quantitative differences between overall cerebellar $GABA_AR$ subunit protein levels in FHM1 R192Q KI cerebellum, compared with age-matched wild-type controls. (C) Representative autoradiograms of [^{3}H] ligand binding to horizontal whole-brain sections of wild-type (left) and R192Q KI (right) mice. Non-specific binding was assessed by competitive binding of non-labeled ligands on wild-type cerebellar sections. (D) Autoradiogram densitometry of three separate experiments did not reveal any statistically significant differences between [^{3}H] $GABA_AR$ ligand binding between wild-type and FHM1 R192Q KI cerebella. (E) [^{3}H] Muscimol binding to control and R192Q KI cerebellar membrane homogenates was similar; no differences in B_{max} and K_D were identified (cf. Table 1). Inset shows Scatchard plot. (F) Similarly, [^{3}H] Ro15-4513 binding was not affected by the R192Q mutation in *Cacna1a*. Inset shows Scatchard plot. Numerical values for binding parameters to wild-type and R192Q KI cerebellar homogenates are provided in Table 2.

homozygous KI mice. Relative quantification using mouse β-actin as endogenous control revealed no statistically significant differences in mRNA levels between wild-type and R192Q KI for the $GABA_A$ receptor subunits α_1, α_6, β_3, γ_2 and δ (n = 6; data not shown). The C_T values obtained and Taqman® assays are presented in Table 1. Similar results were obtained when glyceraldehyde-3-phosphate dehydrogenase was used as endogenous control (data not shown).

We next performed semi-quantitative immunoblotting using antibodies directed against $GABA_A$ receptor subunits (Fig. 1A). We did not identify any statistically

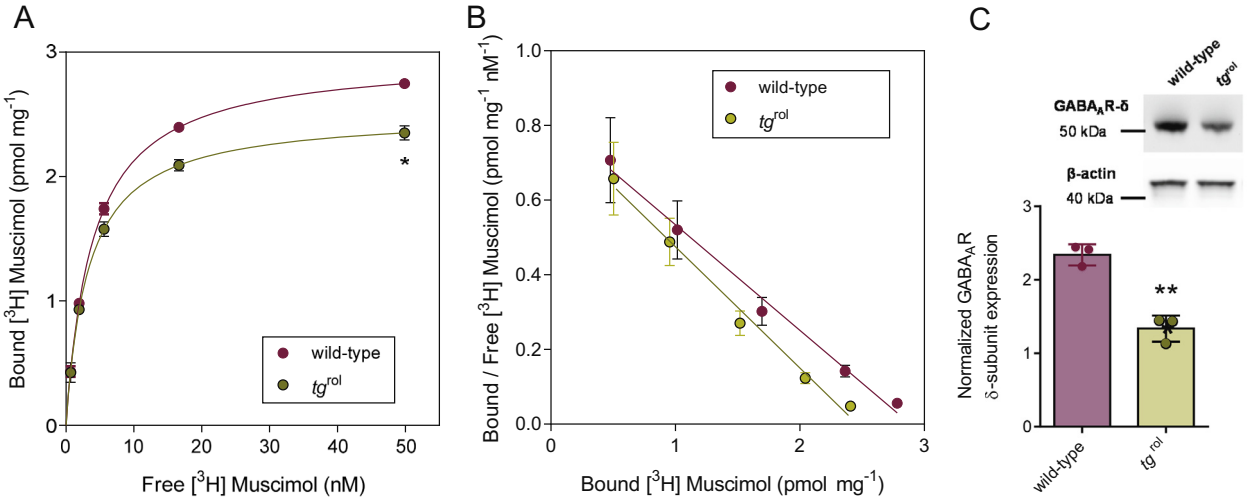

Fig. 2. (A) The number of [^{3}H] muscimol binding sites was reduced by 14% in the cerebellum of *tg*^{rol} mice, compared with wild-type (n = 4; P < 0.05). Binding affinity was similar between wild-type and *tg*^{rol} cerebella (cf. Table 2). (B) Data were transformed using the Rosenthal method and are presented as a Scatchard plot, showing an increase in B_{max} (x-axis intercept) with similar K_D (−1 × slope). (C) Representative immunobands for the GABA$_A$R δ subunit and β-actin. Densitometry revealed a 42.9 ± 4.4% reduction of GABA$_A$R δ subunit expression (normalized to β-actin) in *tg*^{rol} cerebellum compared with wild-type (n = 3, P < 0.01).

Table 1. C_T values

Gene	Subunit	C_T (± S.D.)		Taqman® probe
		Wild-type	R192Q KI	
Gabra1	α_1	25.95 ± 0.70	25.53 ± 0.61	Mm00439040_m1
Gabra6	α_6	25.17 ± 0.45	25.58 ± 0.49	Mm00433456_m1
Gabrb2	β_2	27.43 ± 0.61	27.46 ± 0.63	Mm00433473_m1
Gabrg2	γ_2	28.91 ± 0.72	29.02 ± 0.27	Mm00433489_m1
Gabrd	δ	29.48 ± 0.40	29.80 ± 0.36	Mm00433476_m1
Actb	–	23.77 ± 0.79	23.38 ± 0.65	4352341E

Quantitative PCR analysis reveals no differences in subunit expression in R192Q KI cerebella compared with *wt*. All P values were >0.05. The threshold cycle (C_T) is inversely proportional to the original relative expression level of the gene of interest and used for calculation of the relative gene expression (R_Q) using the $2^{-\Delta\Delta CT}$ method (Livak and Schmittgen, 2001).

significant changes in overall levels of GABA$_A$ receptor subunit proteins between wild-type and R192Q KI cerebella from age-matched animals (Fig. 1B).

Subsequently, we investigated the distribution of known GABA$_A$ receptor subtypes in the cerebellum using [^{3}H] autoradiography on whole-brain sections from wild-type and R192Q KI mice. [^{3}H] Muscimol under these conditions selectively highlights α_6-containing GABA$_A$ receptor populations that are specifically expressed by CGCs ($\alpha_6\beta_x\gamma_2$ and $\alpha_6\beta_x\delta$) (Jones et al., 1997; Mihalek et al., 1999; Kaja et al., 2007a). Fig. 1C shows representative micrographs obtained from wild-type animals and R192Q KI littermates. Quantitative analysis revealed similar densities of [^{3}H] muscimol in CGCs of R192Q KI and wild-type mice (Fig. 1D).

[^{3}H] Ro15-4513 allows the distinction between two α_6-containing receptor subpopulations, specifically $\alpha_6\beta_x\gamma_2$ and $\alpha_6\beta_x\delta$, and the investigation of the $\alpha_1\beta_x\gamma_2$ subtypes. [^{3}H] Ro15-4513 alone highlights γ_2-containing GABA$_A$Rs, i.e. exclusive of δ subunit containing receptors. Pharmacological manipulation using flunitrazepam further allows the separation of benzodiazepine-sensitive $\alpha_1\beta_x\gamma_2$ (BZ-S) and benzodiazepine-insensitive $\alpha_6\beta_x\gamma_2$ (BZ-IS) receptors. Densitometric analysis did not reveal any significant changes in either the abundance or localization of these receptor subtypes (Fig. 1C, D). Lastly, we used the benzodiazepine receptor antagonist [^{3}H] Ro15-1788 (flumazenil). In accordance with our results from [^{3}H] muscimol and [^{3}H] Ro15-4513, the distribution and intensity of GABA$_A$Rs binding were similar in wild-type and R192Q KI cerebella (Fig. 1C, D). The right panel in Fig. 1C shows representative examples of ligand displacement confirming ligand specificity.

In order to quantify functional GABA$_A$Rs, we examined the binding characteristics of GABA$_A$Rs in the cerebellum of wild-type and R192Q KI littermates. Individual cerebella were tested in triplicate against [^{3}H] ligands. [^{3}H] muscimol binds to the GABA site of GABA$_A$Rs and provides an estimate of the total number of functional receptors expressed on cerebellar membranes. Fitting the binding curve using a single binding-site equation revealed no statistically significant

difference between the B_{max} of wild-type and R192Q KI mutant mice (Table 1; Fig. 1E). Rosenthal transformations of the data are presented as Scatchard plot for illustration (Fig. 1E inset). K_D values were similar between genotypes and also similar to those previously reported for cerebellar $GABA_A$Rs (Thompson et al., 1998; Kaja et al., 2007a).

In a similar manner, total benzodiazepine receptor binding was determined using [^{3}H] Ro15-4513 and the B_{max} and K_D values calculated (Table 2). No differences in the total number of functional receptors or binding properties were observed. We excluded the possibility of subunit changes in the composition of $GABA_A$Rs as a result of the R192Q mutation by differentiating BZ-IS, BZ-S and Ro15-1788 binding properties. No differences in B_{max} and K_D values were identified (Table 2).

Reduced $GABA_A$ receptor δ-subunit in *tg*^{rol} mice

As a positive control for radioligand binding assays and to show reproducibility of our experimental setup, we also quantified muscimol binding sites in the cerebellum of *tg* mice to validate the previously reported 40% reduction in $\alpha_6\beta_{2/3}\gamma_2$-containing $GABA_A$Rs in CGCs (Kaja et al., 2007a). In accordance with previous data, we found a 41% reduction in total GABA sites using [^{3}H] muscimol ($n = 4$, $P < 0.001$; Table 2).

We next investigated $GABA_A$R binding sites in the cerebellum of *tg*^{rol} mice. Changes in the *tg*^{rol} cerebellum are particularly interesting, as this particular strain exhibits ataxia without any motor phenotype, and lacks compensatory expression of calcium channels in the cerebellum (Hansen et al., 1992). [^{3}H] muscimol binding revealed a statistically significant 15% reduction in the

Table 2. Binding properties in *Cacna1a* cerebella

R192Q KI		Wild-type	R192Q KI	*n*; *P*
[^{3}H] Muscimol	B_{max}	1.33 ± 0.11	1.37 ± 0.03	$n = 3$; $P = 0.724$
	K_D	2.83 ± 0.32	3.31 ± 0.25	$n = 3$; $P = 0.308$
Total [^{3}H] Ro15-4513	B_{max}	1.90 ± 0.08	1.90 ± 0.12	$n = 3$; $P = 0.972$
	K_D	4.68 ± 0.26	5.34 ± 0.50	$n = 3$; $P = 0.309$
BZ-IS [^{3}H] Ro15-4513	B_{max}	0.92 ± 0.15	0.91 ± 0.07	$n = 3$; $P = 0.940$
	K_D	16.44 ± 3.94	15.90 ± 1.45	$n = 3$; $P = 0.904$
BZ-S [^{3}H] Ro15-4513	B_{max}	1.18 ± 0.10	1.15 ± 0.08	$n = 3$; $P = 0.878$
	K_D	3.13 ± 0.18	3.63 ± 0.32	$n = 3$; $P = 0.255$
[^{3}H] Ro15-1788	B_{max}	0.84 ± 0.16	0.88 ± 0.02	$n = 3$; $P = 0.787$
	K_D	1.36 ± 0.24	1.09 ± 0.03	$n = 3$; $P = 0.333$
Rolling Nagoya		Wild-type	*tg*^{rol}	*n*; *P*
[^{3}H] Muscimol	B_{max}	2.97 ± 0.27	2.51 ± 0.30	$n = 4$; $P < 0.05$
	K_D	3.66 ± 0.03	3.32 ± 0.10	$n = 4$; $P = 0.198$
Total [^{3}H] Ro15-4513	B_{max}	2.34 ± 0.14	2.21 ± 0.17	$n = 4$; $P = 0.563$
	K_D	9.60 ± 0.29	8.61 ± 0.41	$n = 4$; $P = 0.097$
BZ-IS [^{3}H] Ro15-4513	B_{max}	1.78 ± 0.12	1.66 ± 0.09	$n = 4$; $P = 0.453$
	K_D	10.45 ± 0.41	8.98 ± 0.19	$n = 4$; $P < 0.05$
BZ-S [^{3}H] Ro15-4513	B_{max}	0.57 ± 0.04	0.56 ± 0.08	$n = 4$; $P = 0.918$
	K_D	7.68 ± 1.07	8.08 ± 1.65	$n = 4$; $P = 0.845$
[^{3}H] Ro15-1788	B_{max}	0.94 ± 0.05	0.96 ± 0.07	$n = 4$; $P = 0.855$
	K_D	1.19 ± 0.03	1.25 ± 0.08	$n = 4$; $P = 0.506$
Tottering		Wild-type	*tg*	
[^{3}H] Muscimol	B_{max}	2.12 ± 0.11	1.25 ± 0.09	$n = 4$; $P < 0.001$
	K_D	4.43 ± 0.78	5.39 ± 1.34	$n = 4$; $P = 0.205$
FHM1 S218L KI		Wild-type	S218L KI	
[^{3}H] Muscimol	B_{max}	1.13 ± 0.05	1.46 ± 0.11	$n = 4$; $P < 0.05$
	K_D	6.57 ± 0.73	5.31 ± 0.43	$n = 4$; $P = 0.187$
Total [^{3}H] Ro15-4513	B_{max}	0.81 ± 0.13	1.91 ± 0.30	$n = 4$; $P < 0.05$
	K_D	4.53 ± 1.97	5.11 ± 0.77	$n = 4$; $P = 0.794$
[^{3}H] Ro15-1788	B_{max}	1.04 ± 0.09	1.40 ± 0.12	$n = 6$; $P < 0.05$
	K_D	1.43 ± 0.18	1.69 ± 0.34	$n = 6$; $P = 0.502$

Pharmacology of $GABA_A$ receptor binding to cerebellar membranes of *Cacna1a* mutants. There is no statistically significant difference in the number of binding sites (B_{max}) or ligand affinity (K_D) between *wt* and R192Q KI mice. We identified a 15% reduction of muscimol binding sites in *tg*^{rol} cerebellum compared to *wt* controls. In control experiments, *tg* mice showed an ~40% reduction in cerebellar muscimol binding sites, in agreement with our earlier observation (Kaja et al., 2007a). In contrast, the gain-of-function S218L KI mutant had an ~29% increase in functional cerebellar GABA binding sites.

number of functional GABA binding sites of tg^{rol} ($n = 4$, $P < 0.05$; Fig. 2A). Rosenthal transformations of the data presented as Scatchard plot (Fig. 2B) confirm similar K_D values (Table 2). Furthermore, [^{3}H] Ro15-4513 and [^{3}H] Ro15-1788 binding did not reveal any statistically significant differences that could account for the observed loss of muscimol binding sites (Table 2).

Given the selective reduction in [^{3}H] muscimol binding, we performed semi-quantitative immunoblotting for the $GABA_AR$ δ-subunit. Expression levels (normalized to β-actin) were reduced by 42.9 ± 4.4% in tg^{rol} cerebellum compared with wild-type control ($n = 3$; $P < 0.01$; Fig. 2C).

Increased $GABA_A$ receptor expression in gain-of-function S218L KI cerebella

Lastly, we quantified cerebellar $GABA_AR$ expression in gain-of-function FHM1 S218L KI. We observed a statistically significant increase in muscimol binding sites (29%; $n = 4$, $P < 0.05$; Fig. 3A, B; Table 2) in the cerebellum. The binding affinity, expressed as K_D, was not different between S218L KI and wild-type littermates (Table 2). Similar increases were observed for benzodiazepine binding sites as assessed using [^{3}H] Ro15-4513 ($n = 4$; $P < 0.05$; Table 2) and [^{3}H] Ro15-1788 ($n = 6$; $P < 0.05$; Table 2). Binding affinities expressed as K_D values were not different between wild-type and tg^{rol} cerebella (Table 2).

DISCUSSION

In this study, we quantified cerebellar $GABA_A$ receptor expression in R192Q KI, S218L KI and tg^{rol} mice, all of which harbor single missense mutations in the *Cacna1a* gene that encodes the pore-forming α_1 subunit of $Ca_V2.1$ (P/Q-type) calcium channels.

Ataxia, $GABA_A$ receptor expression and Ca^{2+} signaling

The functional link between $GABA_A$ receptor expression and Ca^{2+} signaling has been well established. Specifically, early electron microscopy co-localization studies showed close proximity between low-affinity $GABA_AR$ subunits and L-type and P/Q-type voltage-gated Ca^{2+} channels (Hansen et al., 1992). Furthermore, expression of the δ subunit of the $GABA_AR$ is controlled and maintained by Ca^{2+} influx through voltage-gated Ca^{2+} channels and *N*-methyl-D-aspartate (NMDA) receptor stimulation (Gault and Siegel, 1997, 1998). Similarly, β_2 and β_3 subunits of $GABA_ARs$ are differentially controlled by Ca^{2+}/calmodulin-dependent protein kinase II, which itself is dependent on Ca^{2+} influx (Houston et al., 2007, 2008). Similarly, ataxia has been linked directly to GABAergic neurotransmission. Loss of GABAergic inhibition, resulting from a reduction in functional $GABA_ARs$ may decrease tonic inhibition in cerebellar granule cells (CGCs), leading to ataxia in Angelman syndrome (Egawa et al., 2012). The same mechanism is also the likely pathophysiological cause of ataxia and tremor in mice lacking the GABA transporter subtype 1, resulting in compromised GABA uptake in both CGCs and PCs (Chiu et al., 2005). Together with findings of aberrant cerebellar $GABA_A$ receptor expression in ataxic *Cacna1a* mutants (Yamaguchi et al., 1984; Ogasawara et al., 2001; Kaja et al., 2007a), it is tentative to speculate that GABAergic changes contribute directly to the pathophysiology of cerebellar ataxia.

Normal $GABA_AR$ expression in non-ataxic FHM1 R192Q KI mice

Quantitative PCR and quantitative immunoblotting revealed no significant differences in the $GABA_AR$ mRNA and protein levels in the cerebellum of FHM1

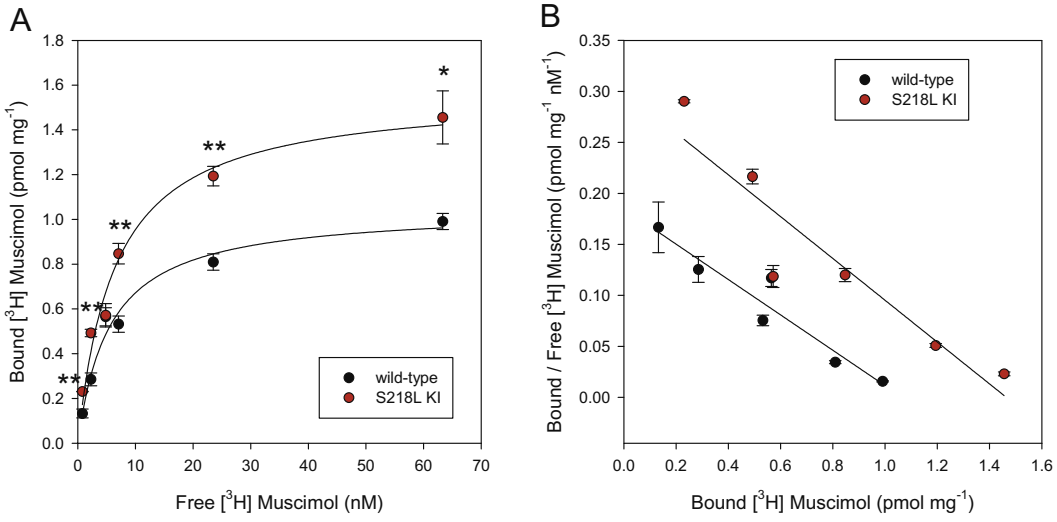

Fig. 3. (A) In contrast to loss-of-function *Cacna1a* mutants, [^{3}H] muscimol binding was increased in S218L KI cerebellar membranes compared with wild-type ($n = 4$, $P < 0.05$), with no apparent change in K_D. (B) Scatchard plot of the Rosenthal transformation of [^{3}H] muscimol binding to S218L KI cerebellar membranes and wild-type control homogenate. Numerical values for binding parameters to wild-type and S218L KI cerebellar homogenates are provided in Table 2.

R192Q KI mice, respectively. We utilized established $GABA_AR$ ligands to investigate receptor pharmacology in the cerebellum of *Cacna1a* mutant mice. Muscimol is a non-selective GABA ligand, which in rapid filtration assays identifies all $GABA_ARs$. In the cerebellum, the major $GABA_AR$ subgroups are $\alpha_1\beta_x\gamma_2$, $\alpha_6\beta_x\gamma_2$ and $\alpha_6\beta_x\delta$ (Poltl et al., 2003). When used as a ligand in autoradiography, muscimol selectively binds to α_6-containing receptors (Jones et al., 1997; Mihalek et al., 1999). [^{3}H] Ro15-4513 and [^{3}H] Ro15-1788 (flumazenil) were used as ligands for the benzodiazepine binding site of $GABA_ARs$, identifying γ_2 subunit-containing receptors (Mohler et al., 1980, 1984). The most predominant $GABA_AR$ subtypes detected by benzodiazepine binding assays in murine cerebella are $\alpha_1\beta_x\gamma_2$, $\alpha_6\beta_x\gamma_2$ and $\alpha_1\alpha_6\beta_x\gamma_2$ receptors (Poltl et al., 2003). Specificity of ligands was confirmed by using 10-fold excess concentrations of unlabeled ligands to displace [^{3}H] ligands, as described previously (Kaja et al., 2007a). In accordance with expression data, quantitative radioligand binding experiments using autoradiography and rapid filtration assays did not reveal any differences between $GABA_AR$ expression in FHM1 R192Q KI and wild-type mice. The B_{max} and K_D values obtained for $GABA_AR$ binding were in accordance with the published literature for mice on the C57/BL6 background (Kaja et al., 2007a).

Reduced expression of the $GABA_AR$ δ subunit in *tg*^{rol} cerebella

In order to adequately compare results for *Cacna1a* mutants, we used cerebella from *tg* mice to repeat our previously reported [^{3}H] muscimol binding. We were able to recapitulate the 40% reduction of muscimol binding in rapid filtration assays, as described previously (Kaja et al., 2007a).

The ataxic *tg*^{rol} strain is a model of cerebellar ataxia, without confounding motor coordination deficits such as dyskinesia or dystonia that are present in for example *tg* mice (Green and Sidman, 1962; Oda, 1973). At the molecular level, the *tg*^{rol} mutation (R1262G) in the domain III voltage-sensor region of the $Ca_V2.1$ protein results in a positive shift of the activation voltage of the channel and reduced current density of the P/Q-type current (Mori et al., 2000), leading to impaired neurotransmission and transmitter secretion (Kaja et al., 2007b; Plomp et al., 2009). One previous study reported an approximately 15% reduction of muscimol binding sites in the *tg*^{rol} cerebellum (Yamaguchi et al., 1984), however no pharmacological dissection was presented. We herein describe a 14.1% reduction in [^{3}H] muscimol binding in rapid filtration assays, while both the total binding (B_{max}) and affinity (K_D) for the benzodiazepine site were unaltered based upon [^{3}H] Ro15-4513 and [^{3}H] Ro15-1788 binding, suggesting a selective reduction in δ subunit-containing $GABA_ARs$. Given that δ subunit-containing receptors constitute an estimated 29% of cerebellar $GABA_ARs$ (Poltl et al., 2003), this decrease represents an approximately 49.0% reduction of these receptors in the *tg*^{rol} cerebellum. In fact, our semi-quantitative immunoblotting detected a 42.9 ± 4.4% reduction in δ subunit expression (Fig. 2C). δ subunits preferentially associate with the BZ-IS α_6 subunit (Jones et al., 1997; Mihalek et al., 1999), and are expressed perisynaptically, where they are activated following GABA spillover in the molecular layer (Wei et al., 2003). Thus, our data suggest a loss of $\alpha_6\beta_x\delta$ receptors, which would likely result in a decrease of tonic GABAergic inhibition (Nusser et al., 1998) in *tg*^{rol} cerebellum. Given the regulation of δ subunit expression by Ca^{2+} influx (Gault and Siegel, 1997), it is tentative to suggest that this reduction is the direct result of reduced Ca^{2+} influx through mutated $Ca_V2.1$ channels.

The total number of GABA and benzodiazepine binding sites (B_{max}) in *tg*^{rol} cerebellum was higher than in FHM1 R192Q KI and *tg* mice. This difference may be explained by different genetic background strains of the various *Cacna1a* strains investigated, as there is evidence in the literature that different genetic backgrounds express different $GABA_A$ receptor profiles (Griebel et al., 2000; Rodgers et al., 2002). Specifically, *tg*^{rol} mice originate from a cross between SIII and C57BL/6J mice maintained on a C3Hf/Nga background (Oda, 1973), compared to R192Q KI mice, which have been backcrossed by more than five generations on the C57BL/6J background (van den Maagdenberg et al., 2004).

Genetic differences in $GABA_AR$ expression may also impact the calculation of the estimated loss of δ subunit-containing $GABA_ARs$ in *tg*^{rol}, as we have relied on data from Poltl et al. (2003), who used a mixed background mouse line C57BL/6J × 129Sv/SvJ. This genetic background is different from the C3Hf/Nga and C57BL/6J background strains, on which *tg*^{rol} and FHM1 KI mice are maintained (Oda, 1973; van den Maagdenberg et al., 2004, 2010). Similar differences in genetic background may also account for the small difference in the number of muscimol binding sites between R192Q KI and S218L KI mice.

Increased number of functional $GABA_ARs$ in S218L KI cerebellum

Unlike all other spontaneous *Cacna1a* mutant strains, FHM1 S218L KI mice display a complex behavioral and synaptic phenotype that includes cerebellar ataxia resulting from a gain-of-function mutation in the $Ca_V2.1$channel (van den Maagdenberg et al., 2010; Gao et al., 2012). In rapid filtration assays, we found a 29% increase in the number of functional $GABA_AR$ binding sites. Furthermore, we detected statistically significant increases in [^{3}H] Ro15-4513 and [^{3}H] Ro15-1788 binding, suggesting an increase in all major cerebellar $GABA_AR$ isoforms, i.e. $\alpha_1\beta_x\gamma_2$, $\alpha_6\beta_x\gamma_2$ and $\alpha_6\beta_x\delta$. Increased presynaptic Ca^{2+} influx as a result of the *Cacna1a* S218L mutation is the likely cause for increased expression of the $GABA_AR$ δ subunit in CGCs (Gault and Siegel, 1997), leading to an increased tonic inhibitory tone and compensatory upregulation of other $GABA_AR$ subunits. More detailed pharmacological studies are needed to dissect the molecular mechanisms of $GABA_AR$ subunit regulation in S218L KI mice.

Pharmaceutical intervention approaches for cerebellar ataxia

Aberrant PC firing has been suggested as the underlying cause of ataxia and dyskinesia (Walter et al., 2006). Specifically, pacemaking in PCs is exclusively controlled by Ca^{2+} influx through $Ca_V2.1$ channels, coupled to small- (SK) and large-conductance (BK) calcium-activated potassium channels (K_{Ca}) (Womack et al., 2004), and it has been postulated that loss-of-function Ca^{2+} channel mutations would result in a reduced activation of K_{Ca} channels, ultimately giving rise to irregular pacemaking of PCs (Walter et al., 2006).

Existing ataxia drugs, acetazolamide and 4-amino pyridine, target this mechanism through direct and indirect effects (Tricarico et al., 2000, 2004; Walter et al., 2006; Alvina and Khodakhah, 2010a,b). Furthermore, several drugs that target SK and BK channels have shown at least some efficacy in both *Cacna1a* loss of function mutants (Walter et al., 2006) and the gain-of-function S218L mutant (Gao et al., 2012). Mice with the *ducky* mutation in *Cacna2d2*, the gene encoding the $\alpha_2\delta$-2 subunit of voltage-gated Ca^{2+} channels, showed improvement of ataxic phenotypes when treated with the SK channel agonist 1-ethyl-2-benzimidazolinone (Walter et al., 2006). Similarly, the selective SK channel agonist NS13001 has shown beneficial effects in mouse models for spinocerebellar ataxia type 2 (Kasumu et al., 2012) and spinocerebellar ataxia type 3 (Shakkottai et al., 2011), suggesting the convergence of distinct signaling mechanisms resulting in aberrant PC pacemaking as the underlying pathology in ataxia.

Yet, there are no existing pharmaceutical intervention approaches that target GABAergic neurotransmission in ataxia despite strong evidence for its involvement in the pathophysiology of ataxia in rodents (Yamaguchi et al., 1984; Payne et al., 2006; Kaja et al., 2007a; present study) and patients (Kish et al., 1983; Perry et al., 1984). Notably, ataxia associated with benzodiazepine treatment is clinically well-established and has recently been linked to the $GABA_AR$ α_1 subunit in rodents, primates and humans (McKernan et al., 2000; Platt et al., 2002; Milic et al., 2012).

CONCLUSION

We herein showed that cerebellar GABAergic changes are a unique feature of *Cacna1a* mutants that display a motor phenotype of ataxia, including tg^{rol} and S218L KI. In contrast, R192Q KI showed normal cerebellar $GABA_AR$ expression. Notably, loss-of-function *Cacna1a* mutations with ataxia resulted in reduced $GABA_AR$ expression, whereas the gain-of-function S218L mutation resulted in an increase in functional $GABA_ARs$. Additional mechanistic studies are needed to establish feasibility for targeting $GABA_AR$ subunits as a novel complementary strategy for cerebellar ataxias that could improve existing treatment approaches with acetazolamide or SK channel activators.

CONFLICT OF INTEREST STATEMENT

The authors declare no actual or potential competing financial interests

Acknowledgements—This work was funded in part by a fellowship from the European Molecular Biology Organization (S.K.), a Michael Smith Foundation for Health Research traineeship (S.K.), the National Headache Foundation (S.K.), an operating grant from the Canadian Institutes of Health Research (#10677) and a Tier 1 Canada Research Chair in Biotechnology and Genomics-Neurobiology (T.P.S.), the Wellcome Trust (grant #066204 to C.L.T.) and the Biotechnology and Biological Sciences Research Council (BBSRC, grant #12/0014803, to C.L.T.), grants EY014227 and EY022774 from NIH/NEI (P.K.), RR022570 from NIH/NCRR (P.K.), AG010485, AG022550 and AG027956 from NIH/NIA (P.K.) as well as by the Felix and Carmen Sabates Missouri Endowed Chair in Vision Research (P.K.), a Challenge Grant from Research to Prevent Blindness (P.K.) and the Vision Research Foundation of Kansas City (P.K.). Excellent technical assistance by Kathrine S. Hansen, Ulla Borberg (both NeuroSearch A/S), Jill Hilgenberg (University of Missouri – Kansas City) and Ray S. Gopaul (University of British Columbia) is gratefully acknowledged. The authors would like to thank Dr. Jaap Plomp (Leiden University Medical Center, Leiden, The Netherlands) for sharing his expertise on Rolling Nagoya mice and Dr. Palle Christophersen (NeuroSearch A/S) for providing his expert advice on potassium channels.

REFERENCES

Alvina K, Khodakhah K (2010a) KCa channels as therapeutic targets in episodic ataxia type-2. J Neurosci 30:7249–7257.

Alvina K, Khodakhah K (2010b) The therapeutic mode of action of 4-aminopyridine in cerebellar ataxia. J Neurosci 30:7258–7268.

Bustin SA, Benes V, Garson JA, Hellemans J, Huggett J, Kubista M, Mueller R, Nolan T, Pfaffl MW, Shipley GL, Vandesompele J, Wittwer CT (2009) The MIQE guidelines: minimum information for publication of quantitative real-time PCR experiments. Clin Chem 55:611–622.

Chiu CS, Brickley S, Jensen K, Southwell A, McKinney S, Cull-Candy S, Mody I, Lester HA (2005) GABA transporter deficiency causes tremor, ataxia, nervousness, and increased GABA-induced tonic conductance in cerebellum. J Neurosci 25:3234–3245.

de Vries B, Frants RR, Ferrari MD, van den Maagdenberg AM (2009) Molecular genetics of migraine. Hum Genet 126:115–132.

Egawa K, Kitagawa K, Inoue K, Takayama M, Takayama C, Saitoh S, Kishino T, Kitagawa M, Fukuda A (2012) Decreased tonic inhibition in cerebellar granule cells causes motor dysfunction in a mouse model of Angelman syndrome. Sci Transl Med 4. 163ra57.

Gao Z, Todorov B, Barrett CF, van Dorp S, Ferrari MD, van den Maagdenberg AM, De Zeeuw CI, Hoebeek FE (2012) Cerebellar ataxia by enhanced Ca(V)2.1 currents is alleviated by Ca2+-dependent K+-channel activators in Cacna1a(S218L) mutant mice. J Neurosci 32:15533–15546.

Gault LM, Siegel RE (1997) Expression of the GABAA receptor delta subunit is selectively modulated by depolarization in cultured rat cerebellar granule neurons. J Neurosci 17:2391–2399.

Gault LM, Siegel RE (1998) NMDA receptor stimulation selectively initiates GABA(A) receptor delta subunit mRNA expression in cultured rat cerebellar granule neurons. J Neurochem 70:1907–1915.

Green MC, Sidman RL (1962) Tottering – a neuromusclar mutation in the mouse. And its linkage with oligosyndacylism. J Hered 53:233–237.

Griebel G, Belzung C, Perrault G, Sanger DJ (2000) Differences in anxiety-related behaviours and in sensitivity to diazepam in inbred and outbred strains of mice. Psychopharmacology 148:164–170.
Hansen GH, Belhage B, Schousboe A (1992) First direct electron microscopic visualization of a tight spatial coupling between GABAA-receptors and voltage-sensitive calcium channels. Neurosci Lett 137:14–18.
Herrup K, Wilczynski SL (1982) Cerebellar cell degeneration in the leaner mutant mouse. Neuroscience 7:2185–2196.
Houston CM, Hosie AM, Smart TG (2008) Distinct regulation of beta2 and beta3 subunit-containing cerebellar synaptic GABAA receptors by calcium/calmodulin-dependent protein kinase II. J Neurosci 28:7574–7584.
Houston CM, Lee HH, Hosie AM, Moss SJ, Smart TG (2007) Identification of the sites for CaMK-II-dependent phosphorylation of GABA(A) receptors. J Biol Chem 282:17855–17865.
Imbrici P, Jaffe SL, Eunson LH, Davies NP, Herd C, Robertson R, Kullmann DM, Hanna MG (2004) Dysfunction of the brain calcium channel CaV2.1 in absence epilepsy and episodic ataxia. Brain 127:2682–2692.
Jen JC, Graves TD, Hess EJ, Hanna MG, Griggs RC, Baloh RW (2007) Primary episodic ataxias: diagnosis, pathogenesis and treatment. Brain 130:2484–2493.
Jones A, Korpi ER, McKernan RM, Pelz R, Nusser Z, Makela R, Mellor JR, Pollard S, Bahn S, Stephenson FA, Randall AD, Sieghart W, Somogyi P, Smith AJ, Wisden W (1997) Ligand-gated ion channel subunit partnerships: GABAA receptor alpha6 subunit gene inactivation inhibits delta subunit expression. J Neurosci 17:1350–1362.
Jouvenceau A, Eunson LH, Spauschus A, Ramesh V, Zuberi SM, Kullmann DM, Hanna MG (2001) Human epilepsy associated with dysfunction of the brain P/Q-type calcium channel. Lancet 358:801–807.
Kaja S, Hann V, Payne HL, Thompson CL (2007a) Aberrant cerebellar granule cell-specific GABAA receptor expression in the epileptic and ataxic mouse mutant, Tottering. Neuroscience 148:115–125.
Kaja S, van de Ven RC, van Dijk JG, Verschuuren JJ, Arahata K, Frants RR, Ferrari MD, Van Den Maagdenberg AM, Plomp JJ (2007b) Severely impaired neuromuscular synaptic transmission causes muscle weakness in the Cacna1a-mutant mouse rolling Nagoya. Eur J Neurosci 25:2009–2020.
Kang JQ, Shen W, Macdonald RL (2006) Why does fever trigger febrile seizures? GABAA receptor gamma2 subunit mutations associated with idiopathic generalized epilepsies have temperature-dependent trafficking deficiencies. J Neurosci 26:2590–2597.
Kasumu AW, Hougaard C, Rode F, Jacobsen TA, Sabatier JM, Eriksen BL, Strobaek D, Liang X, Egorova P, Vorontsova D, Christophersen P, Ronn LC, Bezprozvanny I (2012) Selective positive modulator of calcium-activated potassium channels exerts beneficial effects in a mouse model of spinocerebellar ataxia type 2. Chem Biol 19:1340–1353.
Kish SJ, Perry TL, Hornykiewicz O (1983) Increased GABA receptor binding in dominantly-inherited cerebellar ataxias. Brain Res 269:370–373.
Kors EE, Terwindt GM, Vermeulen FL, Fitzsimons RB, Jardine PE, Heywood P, Love S, Van Den Maagdenberg AM, Haan J, Frants RR, Ferrari MD (2001) Delayed cerebral edema and fatal coma after minor head trauma: role of the CACNA1A calcium channel subunit gene and relationship with familial hemiplegic migraine. Ann Neurol 49:753–760.
Kotagal V (2012) Acetazolamide-responsive ataxia. Semin Neurol 32:533–537.
Livak KJ, Schmittgen TD (2001) Analysis of relative gene expression data using real-time quantitative PCR and the 2(-Delta Delta C(T)) Method. Methods 25:402–408.
Lowry OH, Rosebrough NJ, Farr AL, Randall RJ (1951) Protein measurement with the Folin phenol reagent. J Biol Chem 193:265–275.
Matsuoka H, Harada K, Endo Y, Warashina A, Doi Y, Nakamura J, Inoue M (2008) Molecular mechanisms supporting a paracrine role of GABA in rat adrenal medullary cells. J Physiol 586:4825–4842.
McKernan RM, Rosahl TW, Reynolds DS, Sur C, Wafford KA, Atack JR, Farrar S, Myers J, Cook G, Ferris P, Garrett L, Bristow L, Marshall G, Macaulay A, Brown N, Howell O, Moore KW, Carling RW, Street LJ, Castro JL, Ragan CI, Dawson GR, Whiting PJ (2000) Sedative but not anxiolytic properties of benzodiazepines are mediated by the GABA(A) receptor alpha1 subtype. Nat Neurosci 3:587–592.
Mehta AK, Ticku MK (1999) Prevalence of the GABAA receptor assemblies containing alpha1-subunit in the rat cerebellum and cerebral cortex as determined by immunoprecipitation: lack of modulation by chronic ethanol administration. Brain Res Mol Brain Res 67:194–199.
Mihalek RM, Banerjee PK, Korpi ER, Quinlan JJ, Firestone LL, Mi ZP, Lagenaur C, Tretter V, Sieghart W, Anagnostaras SG, Sage JR, Fanselow MS, Guidotti A, Spigelman I, Li Z, DeLorey TM, Olsen RW, Homanics GE (1999) Attenuated sensitivity to neuroactive steroids in gamma-aminobutyrate type A receptor delta subunit knockout mice. Proc Natl Acad Sci U S A 96:12905–12910.
Milic M, Divljakovic J, Rallapalli S, van Linn ML, Timic T, Cook JM, Savic MM (2012) The role of alpha1 and alpha5 subunit-containing GABAA receptors in motor impairment induced by benzodiazepines in rats. Behav Pharmacol 23:191–197.
Mohler H, Battersby MK, Richards JG (1980) Benzodiazepine receptor protein identified and visualized in brain tissue by a photoaffinity label. Proc Natl Acad Sci U S A 77:1666–1670.
Mohler H, Sieghart W, Richards JG, Hunkeler W (1984) Photoaffinity labeling of benzodiazepine receptors with a partial inverse agonist. Eur J Pharmacol 102:191–192.
Mori Y, Wakamori M, Oda S, Fletcher CF, Sekiguchi N, Mori E, Copeland NG, Jenkins NA, Matsushita K, Matsuyama Z, Imoto K (2000) Reduced voltage sensitivity of activation of P/Q-type Ca2+ channels is associated with the ataxic mouse mutation rolling Nagoya (tg(rol)). J Neurosci 20:5654–5662.
Nusser Z, Sieghart W, Somogyi P (1998) Segregation of different GABAA receptors to synaptic and extrasynaptic membranes of cerebellar granule cells. J Neurosci 18:1693–1703.
Oda S (1973) The observation of rolling mouse Nagoya (rol), a new neurological mutant, and its maintenance (author's transl). Jikken Dobutsu 22:281–288.
Ogasawara M, Kurihara T, Hu Q, Tanabe T (2001) Characterization of acute somatosensory pain transmission in P/Q-type Ca(2+) channel mutant mice, leaner. FEBS Lett 508:181–186.
Ophoff RA, Terwindt GM, Vergouwe MN, van Eijk R, Oefner PJ, Hoffman SM, Lamerdin JE, Mohrenweiser HW, Bulman DE, Ferrari M, Haan J, Lindhout D, van Ommen GJ, Hofker MH, Ferrari MD, Frants RR (1996) Familial hemiplegic migraine and episodic ataxia type-2 are caused by mutations in the Ca2+ channel gene CACNL1A4. Cell 87:543–552.
Pandolfo M, Manto M (2013) Cerebellar and afferent ataxias. Continuum (Minneap Minn) 19:1312–1343.
Payne HL, Donoghue PS, Connelly WM, Hinterreiter S, Tiwari P, Ives JH, Hann V, Sieghart W, Lees G, Thompson CL (2006) Aberrant GABA(A) receptor expression in the dentate gyrus of the epileptic mutant mouse stargazer. J Neurosci 26:8600–8608.
Perry TL, Kish SJ, Hinton D, Hansen S, Becker LE, Gelfand EW (1984) Neurochemical abnormalities in a patient with ataxia-telangiectasia. Neurology 34:187–191.
Platt DM, Rowlett JK, Spealman RD, Cook J, Ma C (2002) Selective antagonism of the ataxic effects of zolpidem and triazolam by the GABAA/alpha1-preferring antagonist beta-CCt in squirrel monkeys. Psychopharmacology 164:151–159.
Plomp JJ, van den Maagdenberg AM, Kaja S (2009) The ataxic Cacna1a-mutant mouse rolling nagoya: an overview of neuromorphological and electrophysiological findings. Cerebellum 8:222–230.
Poltl A, Hauer B, Fuchs K, Tretter V, Sieghart W (2003) Subunit composition and quantitative importance of GABA(A) receptor subtypes in the cerebellum of mouse and rat. J Neurochem 87:1444–1455.

Rodgers RJ, Davies B, Shore R (2002) Absence of anxiolytic response to chlordiazepoxide in two common background strains exposed to the elevated plus-maze: importance and implications of behavioural baseline. Genes Brain Behav 1:242–251.

Shakkottai VG, do Carmo Costa M, Dell'Orco JM, Sankaranarayanan A, Wulff H, Paulson HL (2011) Early changes in cerebellar physiology accompany motor dysfunction in the polyglutamine disease spinocerebellar ataxia type 3. J Neurosci 31:13002–13014.

Stam AH, Luijckx GJ, Poll-The BT, Ginjaar IB, Frants RR, Haan J, Ferrari MD, Terwindt GM, van den Maagdenberg AM (2009) Early seizures and cerebral oedema after trivial head trauma associated with the CACNA1A S218L mutation. J Neurol Neurosurg Psychiatry 80:1125–1129.

Thompson CL, Tehrani MH, Barnes Jr EM, Stephenson FA (1998) Decreased expression of GABAA receptor alpha6 and beta3 subunits in stargazer mutant mice: a possible role for brain-derived neurotrophic factor in the regulation of cerebellar GABAA receptor expression? Brain Res Mol Brain Res 60:282–290.

Tricarico D, Barbieri M, Camerino DC (2000) Acetazolamide opens the muscular KCa2+ channel: a novel mechanism of action that may explain the therapeutic effect of the drug in hypokalemic periodic paralysis. Ann Neurol 48:304–312.

Tricarico D, Barbieri M, Mele A, Carbonara G, Camerino DC (2004) Carbonic anhydrase inhibitors are specific openers of skeletal muscle BK channel of K+-deficient rats. FASEB J 18:760–761.

van den Maagdenberg AM, Pietrobon D, Pizzorusso T, Kaja S, Broos LA, Cesetti T, van de Ven RC, Tottene A, van der Kaa J, Plomp JJ, Frants RR, Ferrari MD (2004) A Cacna1a knockin migraine mouse model with increased susceptibility to cortical spreading depression. Neuron 41:701–710.

van den Maagdenberg AM, Pizzorusso T, Kaja S, Terpolilli N, Shapovalova M, Hoebeek FE, Barrett CF, Gherardini L, van de Ven RC, Todorov B, Broos LA, Tottene A, Gao Z, Fodor M, De Zeeuw CI, Frants RR, Plesnila N, Plomp JJ, Pietrobon D, Ferrari MD (2010) High cortical spreading depression susceptibility and migraine-associated symptoms in Ca(v)2.1 S218L mice. Ann Neurol 67:85–98.

Walter JT, Alvina K, Womack MD, Chevez C, Khodakhah K (2006) Decreases in the precision of Purkinje cell pacemaking cause cerebellar dysfunction and ataxia. Nat Neurosci 9:389–397.

Wei W, Zhang N, Peng Z, Houser CR, Mody I (2003) Perisynaptic localization of delta subunit-containing GABA(A) receptors and their activation by GABA spillover in the mouse dentate gyrus. J Neurosci 23:10650–10661.

Womack MD, Chevez C, Khodakhah K (2004) Calcium-activated potassium channels are selectively coupled to P/Q-type calcium channels in cerebellar Purkinje neurons. J Neurosci 24:8818–8822.

Yamaguchi T, Hayashi K, Murakami H, Maruyama S, Yamaguchi M (1984) Distribution and characterization of the GABA receptors in the CNS of ataxic mutant mouse. Neurochem Res 9:485–495.

Zhuchenko O, Bailey J, Bonnen P, Ashizawa T, Stockton DW, Amos C, Dobyns WB, Subramony SH, Zoghbi HY, Lee CC (1997) Autosomal dominant cerebellar ataxia (SCA6) associated with small polyglutamine expansions in the alpha 1A-voltage-dependent calcium channel. Nat Genet 15:62–69.

(Accepted 13 July 2015)
(Available online 21 July 2015)